

Luminescence quenching in erbium-doped hydrogenated amorphous silicon

Jung H. Shin, R. Serna, G. N. van den Hoven, and A. Polman
FOM Institute for Atomic and Molecular Physics, Kruislaan 407, 1098 SJ Amsterdam, the Netherlands

W. G. J. H. M. van Sark and A. M. Vredenberg
Department of Atomic and Interface Physics, Debye Institute, University of Utrecht, P. O. Box 80000,
3508 TA Utrecht, the Netherlands

(Received 3 October 1995; accepted for publication 19 October 1995)

Hydrogenated amorphous silicon thin films are doped with erbium by ion implantation. Room-temperature photoluminescence at $1.54\ \mu\text{m}$, due to an intra- $4f$ transition in Er^{4+} , is observed after thermal annealing at $300\text{--}400\ \text{C}$. Excitation of Er^{3+} is shown to be mediated by photocarriers. The Er^{3+} luminescence intensity is quenched by a factor of 15 as the temperature is raised from 10 K to room temperature. Codoping with oxygen (1 at. %) reduces the luminescence quenching to a factor of 7. The quenching is well correlated with a decrease in luminescence lifetime, indicating that nonradiative decay of excited Er^{3+} is the dominant quenching mechanism as the temperature is increased. © 1996 American Institute of Physics. [S0003-6951(96)01001-7]

Erbium-doped materials can emit light at $1.54\ \mu\text{m}$, due to an intra- $4f$ shell transition from the first excited ($^4I_{13/2}$) to the ground ($^4I_{15/2}$) state of the Er^{3+} ion. As this wavelength coincides with the low-loss window of silica-based optical fibers, and the luminescence wavelength is largely independent of host material and temperature, a large amount of research activity is being devoted to the study of Er-doped materials for potential use in optoelectronic components.¹ Especially, Er-doped silicon is under intensive investigation as a possible silicon-based light source,² circumventing the inefficiency of silicon in generating light due to its indirect band gap. Recently, room temperature photoluminescence³⁻⁵ and electroluminescence^{6,7} of Er-doped crystalline Si (*c*-Si) have been reported.

Another promising host material for Er is amorphous silicon. Being amorphous, it allows one to sidestep the problem of limited solubility of Er in crystalline semiconductors,^{8,9} and to incorporate more of the impurities such as oxygen and carbon that are known to enhance the luminescence.^{3,5,10} Our earlier work on Er doping of pure amorphous Si has shown luminescence only at low temperature (77 K).¹¹ More recent experiments have shown that room-temperature photoluminescence¹² and electroluminescence¹³ can be achieved from heavily oxygen-doped (30 at. %) amorphous Si (SIPOS). The disadvantage of this material is that its electrical quality is rather poor, and it is therefore interesting to investigate amorphous materials with better electrical quality.

Hydrogenated amorphous Si (*a*-Si:H) is such a material; it is a well characterized, mature semiconductor, with the possibility of direct deposition on optical materials, and shows excellent electrical properties. In this letter, we present a photoluminescence characterization of device-quality *a*-Si:H films doped with Er by ion implantation. These films show room-temperature $1.54\ \mu\text{m}$ photoluminescence from Er^{3+} , with an intensity higher than what has been achieved in *c*-Si so far. The excitation mechanism and temperature dependence of the luminescence of Er in *a*-Si:H are

studied, as well as the effect of oxygen codoping.

A 250 nm thick *a*-Si:H film was deposited on glass (Corning 7059) by plasma enhanced chemical vapor deposition (PECVD) of SiH_4 at $230\ \text{C}$. The H content in the films was 10 at. %, and a background concentration of 0.3 at. % O was also present, as measured using elastic recoil spectrometry. Erbium was implanted at 125 keV to a dose of $4 \times 10^{14}\ \text{Er}/\text{cm}^2$, corresponding to a peak concentration of 0.2 at. %. In some samples, additional O was implanted at 25 keV to a dose of $7 \times 10^{15}\ \text{O}/\text{cm}^2$, corresponding to a peak O concentration of 1.0 at. %, which overlaps with the Er profile. The Er-doped samples with the two different O contents will be referred to as the low-O and high-O samples, respectively. After implantation, samples were annealed in vacuum for 2 h. Photoluminescence (PL) spectra were measured using the 515 nm line of an Ar laser as the excitation source at a nominal power of 50 mW. A closed-cycle helium cryostat was used for low temperature measurements. PL excitation spectroscopy was performed using the lines of the Ar laser in the wavelength range 455–515 nm.

Figure 1 shows the room-temperature PL spectra of Er-implanted *a*-Si:H samples (low O and high O), annealed at $400\ \text{C}$, displaying characteristic Er^{3+} luminescence at $1.54\ \mu\text{m}$. The inset shows the Er^{3+} luminescence intensity at $1.54\ \mu\text{m}$ as a function of the annealing temperature. As can be seen, samples annealed at $300\text{--}400\ \text{C}$ display the optimum Er^{3+} luminescence. Therefore, these were chosen for all further studies. No erbium-related luminescence can be observed from either the as-implanted samples nor from the samples annealed at $500\ \text{C}$. The increasing and decreasing trends in the inset are attributed to the competing effects of removal of irradiation-induced defects and out-diffusion of hydrogen as the annealing temperature is increased. Hydrogen is essential for passivating the defects inherent in *a*-Si:H. It has been shown before that Er in pure *a*-Si without hydrogen does not luminesce at room temperature.¹¹ The room-temperature PL intensity for the high-O sample is more than two orders of magnitude larger than that for Er-doped *c*-Si

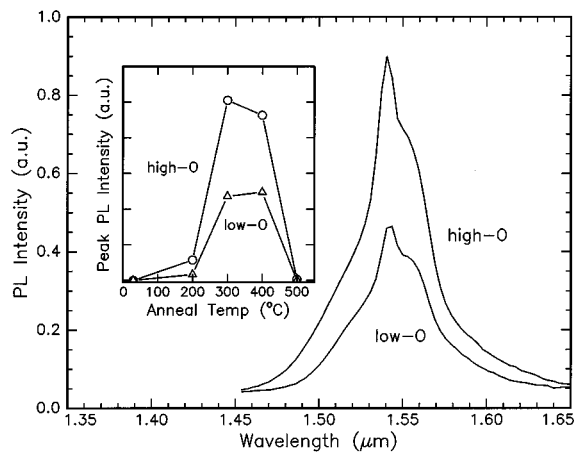


FIG. 1. Room-temperature photoluminescence spectra of Er-implanted *a*-Si:H with two different O contents: low O (0.3 at. %) and high O (1.3 at. %). The Er fluence was 4×10^{14} Er/cm² and both samples were annealed at 400 °C. The inset shows the peak intensity at 1.54 μm at room temperature as function of the anneal temperature for both samples.

codoped with oxygen and annealed for optimum luminescence, and measured under identical conditions.

Figure 2 shows the peak intensity at 1.54 μm as a function of excitation wavelength for the two samples in Fig. 1. A measurement for an Er-implanted SiO₂ sample (1.9×10^{15} Er/cm², annealed at 900 °C) is also shown. For the latter sample, the excitation spectrum shows distinct peaks near the pump wavelengths of 488 and 514 nm, reflecting the $^4I_{15/2} \rightarrow ^4F_{7/2}$ and $^4I_{15/2} \rightarrow ^2H_{11/2}$ optical absorption bands of Er³⁺, respectively. In contrast, the Er³⁺ luminescence in *a*-Si:H does not show such structure, indicating that excitation of Er in *a*-Si:H is photocarrier-mediated rather than through direct optical absorption. Such an excitation process involves recombination of electron-hole pairs trapped at an Er-related defect level in the Si bandgap, followed by transfer of the carrier recombination energy to the Er³⁺ ion through an impurity-Auger transition, as is schematically indicated in the inset in Fig. 3.

Figure 3 shows high resolution PL spectra, measured at 10 K, for the Er-implanted *a*-Si:H samples (low O and high

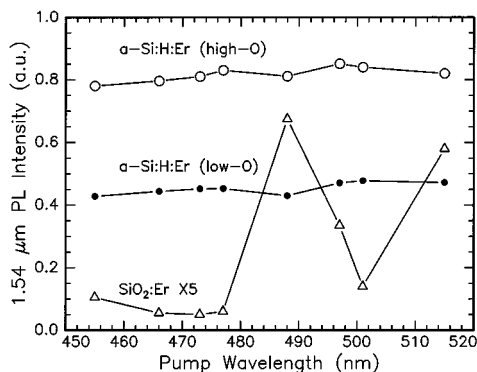


FIG. 2. Photoluminescence excitation spectra of *a*-Si:H (low O and high O) implanted with 4×10^{14} Er/cm² and annealed at 400 °C, and of Er-implanted SiO₂ (1.9×10^{15} Er/cm² + 900 °C). The Er³⁺ luminescence intensity at 1.54 μm is plotted vs the excitation wavelength. All data were taken at room temperature at a constant pump power of 50 mW.

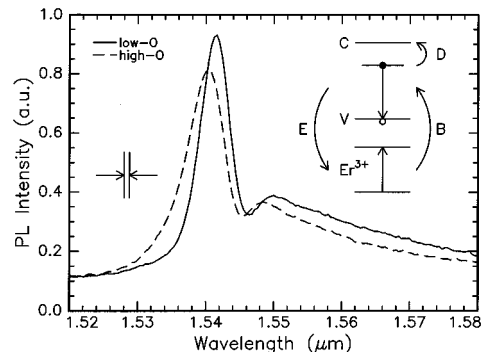


FIG. 3. Photoluminescence spectra of Er-implanted *a*-Si:H (low O and high O, both annealed at 400 °C), measured at 10 K. $\lambda_{\text{pump}} = 515$ nm, pump power = 50 mW. The resolution was 0.8 nm. The inset shows a schematic of the Er excitation process (arrow “E”). “C” and “V” denote the Si conduction and valence bands; “D” and “B” the detrapping and backtransfer quenching mechanisms.

O). For both samples the peaks are broad, indicating the lack of well-defined sites in *a*-Si:H. Unlike at room temperature (see Fig. 1), the integrated luminescence intensities for both samples are nearly identical. There exists a clear difference, however, between the peak position of both spectra, indicating that the presence of additional O changes the local environment of Er. A similar peak shift due to the addition of O has also been observed in *c*-Si.¹⁰ In *c*-Si it has been shown that Er is a microscopic getter for O,¹⁴ and the effective solubility of Er in *c*-Si may be entirely determined by the O content.^{8,9} The data in Fig. 3 does indicate that such Er–O cluster formation also takes place in *a*-Si:H.

Time-resolved measurements at 10 K of the luminescence intensity upon start and termination of a short laser pulse (not shown) have indicated that both the excitation and de-excitation rate of Er are the same for the two samples in Fig. 3. Together with the nearly identical luminescence intensity at 10 K, this implies that the density of optically active Er ions is the same in both samples. Thus, the difference in PL intensity at room temperature must be due to differences in the temperature dependence of the excitation or de-excitation rate for both samples.

Figure 4 shows the temperature dependence of the integrated Er³⁺ luminescence intensity and lifetime for the Er-implanted low-O *a*-Si:H sample. The inset shows the data above 160 K in detail, as well as data for the high-O sample. All intensity data are normalized to the value at 10 K. Between 10 and 110 K, the integrated Er³⁺ PL intensity shows a slight increase as the temperature increases. At the same time, the lifetime decreases. Above 110 K, a 15-fold reduction in the Er³⁺ luminescence intensity is observed as the temperature is increased to 300 K. Up to 250 K, the temperature quenching of the Er³⁺ luminescence intensity correlates well with that of the lifetime (see inset in Fig. 4). No lifetime measurements could be made at temperatures greater than 250 K as it became shorter than the system response time (30 μs). However, extrapolating the lifetime data to higher temperatures, it becomes clear that the intensity quenching nearly fully correlates with the lifetime quenching. The high-O sample shows less quenching (only a factor of 7 between 10 and 300 K), and again the trend in the intensity is

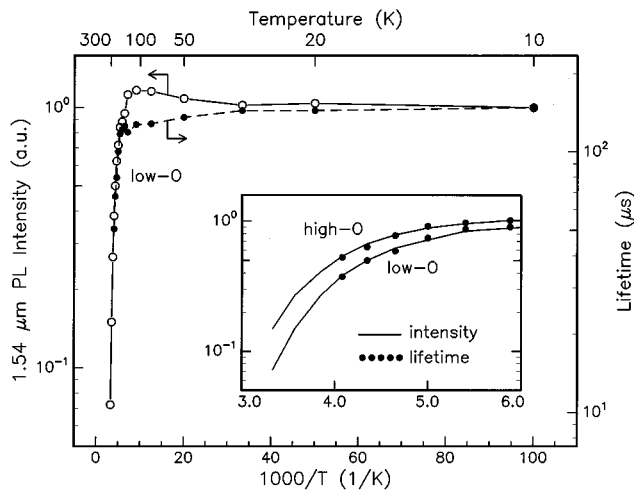


FIG. 4. Arrhenius plot of the normalized, integrated luminescence intensity (open circles and solid line) and lifetime (filled circles and dashed line) of Er-implanted *a*-Si:H (low O). The inset shows the same curves in a smaller temperature range. Data for the high-O sample are also shown in the inset. In order to compare trends in intensity and lifetime, the lifetime data in the inset are normalized to the intensity data at $1000/T=6.0$.

very well correlated with the change in lifetime.

In general, the quenching of the luminescence intensity in Er-doped Si, as the temperature is increased, can be a result of two distinct processes: (1) a reduction in the *excitation rate* of Er^{3+} due to detrapping of electrical carriers trapped at the Er-related level in the Si (arrow “D” in Fig. 3).¹⁰ (2) An increase in the *de-excitation rate* of excited Er^{3+} due to coupling to defect levels in the Si band gap, e.g., to the Er-related defect (i.e., backtransfer, the inverse of the excitation process, see arrow “B” in Fig. 3).¹² These nonradiative processes decrease the luminescence lifetime as well as the intensity at increased temperature.

The correlation between the intensity and lifetime data above 110 K in Fig. 4 shows that the decreased lifetime, i.e., increased de-excitation, can fully explain the quenching of the Er luminescence intensity in *a*-Si:H. This implies that there is no temperature dependence in the excitation rate, i.e., mechanism (1) (arrow “D”) is not effective in *a*-Si:H. This contrasts with the behavior of Er in crystalline Si, where it has been argued that the carrier detrapping effect is important.¹⁰ Consequently, the Er-related level is positioned deeper in the forbidden gap in *a*-Si:H than in *c*-Si. Given the fact that the band gap of *a*-Si:H (1.6 eV) is larger than of *c*-Si (1.1 eV), this is plausible. Our data also correlate with previous work on III–V and II–VI semiconductors doped with Er,¹⁵ as well as Er-doped SIPOS,¹² that has shown the trend that the quenching is reduced as the band gap is increased.

Figure 4 also shows that O co-doping reduces the quenching, as it does in *c*-Si.¹⁰ For the highest O content studied in crystalline Si (0.2 at. %), the quench factor between 77 and 300 K was 30.¹⁰ However, in this case the

absolute PL intensity was lower than for samples with lower O content, presumably due to a reduction in minority carrier lifetime due to the high O content. In contrast, in *a*-Si:H the O content can be increased to at least 1.3 at. % (high-O sample), causing a further reduction in the quenching to only a factor of 7. This shows the advantage of an amorphous host in accommodating large concentrations of impurities such as Er and O. Note that the Er-doped high-O sample in Fig. 1 showed two orders of magnitude more intensity than a comparable *c*-Si sample. This difference is partly ascribed to the higher optical absorption coefficient of *a*-Si, leading to higher carrier densities in the Er-implanted region.

In conclusion, we have observed room-temperature 1.54 μm photoluminescence from Er-implanted *a*-Si:H, codoped with O at two different concentrations (0.3 and 1.3 at. %). The excitation is mediated by photocarriers. In the low-O sample the luminescence intensity is quenched by a factor of 15 as the temperature is raised from 10 K to room temperature, primarily due to an increase in the de-excitation rate of excited Er^{3+} . Additional oxygen does not increase the optically active Er concentration, but does reduce the luminescence quenching at increased temperature.

C. H. M. van der Werf is acknowledged for depositing the *a*-Si:H films. F. W. Saris is acknowledged for critical reading of the manuscript. This work is part of the research program of FOM and made possible by financial support from NWO, STW, and IOP-Electro Optics.

¹ See, for example, *Rare Earth Doped Semiconductors*, edited by G. S. Pomrenke, P. B. Klein, and D. W. Langer, Mater. Res. Soc. Symp. Proc. **301** (1993).

² H. Ennen, J. Schneider, G. Pomrenke, and A. Axmann, Appl. Phys. Lett. **43**, 943 (1983).

³ J. Michel, J. L. Benton, R. F. Ferrante, D. C. Jacobson, D. J. Eaglesham, E. A. Fitzgerald, Y. H. Xie, J. M. Poate, and L. C. Kimerling, J. Appl. Phys. **70**, 2672 (1991).

⁴ R. Serna, E. Snoeks, G. N. van den Hoven, and A. Polman, J. Appl. Phys. **75**, 2644 (1994).

⁵ S. Coffa, G. Franzò, F. Priolo, A. Polman, and R. Serna, Phys. Rev. B **49**, 16313 (1994).

⁶ G. Franzò, F. Priolo, S. Coffa, A. Polman, and A. Carnera, Appl. Phys. Lett. **64**, 2235 (1994).

⁷ B. Zhen, J. Michel, F. Y. G. Ren, L. C. Kimerling, D. C. Jacobson, and J. M. Poate, Appl. Phys. Lett. **64**, 2842 (1994).

⁸ D. J. Eaglesham, J. Michel, E. A. Fitzgerald, D. C. Jacobson, J. M. Poate, J. L. Benton, A. Polman, Y.-H. Xie, and L. C. Kimerling, Appl. Phys. Lett. **58**, 2797 (1991).

⁹ A. Polman, G. N. Van den Hoven, J. S. Custer, J. H. Shin, R. Serna, and P. F. A. Alkemade, J. Appl. Phys. **77**, 1256 (1995).

¹⁰ F. Priolo, G. Franzò, S. Coffa, A. Polman, S. Libertino, R. Barklie, and D. Carey, J. Appl. Phys. **78**, 3874 (1995).

¹¹ J. S. Custer, E. Snoeks, and A. Polman, Mater. Res. Soc. Symp. Proc. **235**, 51 (1992).

¹² G. N. van den Hoven, Jung H. Shin, A. Polman, S. Lombardo, and S. U. Campisano, J. Appl. Phys. **78**, 2642 (1995).

¹³ S. Lombardo, S. U. Campisano, G. N. van den Hoven, and A. Polman, J. Appl. Phys. **77**, 6504 (1995).

¹⁴ D. L. Adler, D. C. Jacobson, D. J. Eaglesham, M. A. Marcus, J. L. Benton, J. M. Poate, and P. H. Citrin, Appl. Phys. Lett. **61**, 2181 (1992).

¹⁵ P. N. Favennec, H. L’Haridon, D. Moutonnet, M. Salvi, and M. Ganneau, Mater. Res. Soc. Symp. Proc. **301**, 181 (1993).